17th World Conference on Earthquake Engineering, 17WCEE
Sendai, Japan - September 13th to 18th 2020

EXPERIMENTAL STUDY ON BUCKLING RESTRAINED BRACES WITH POST-TENSIONED CARBON FIBER COMPOSITE CABLES

K. Atasever [1], S. Inanaga [2], Y. Terazawa [3], T. Takeuchi [4], O.C. Celik [5]

[1] *Research Assistant, Mimar Sinan Fine Arts University, kurtulus.atasever@msgsu.edu.tr*
[2] *Graduate Student, Tokyo Institute of Technology, inanaga.s.aa@m.titech.ac.jp*
[3] *Assistant Professor, Tokyo Institute of Technology, terazawa.y.aa@m.titech.ac.jp*
[4] *Professor, Tokyo Institute of Technology, takeuchi.t.ab@m.titech.ac.jp*
[5] *Professor, Istanbul Technical University, celikoguz@itu.edu.tr*

Abstract

Seismic performance of buildings is generally evaluated by peak values of drift/displacement response to assure life safety performance level. Residual deformation following a strong earthquake is a significant indicator to make a decision whether existing buildings could be operational or not. Final condition of structures with higher importance factors such as hospitals, schools, bridges etc. is expected to be operational after a design basis earthquake (DBE). Previous researchers showed that post-yield stiffness for bilinear hysteretic behavior or post-tensioning force for flag shaped hysteretic behavior are highly effective in reducing such residual deformations. Also, fully self-centering behavior may be not necessary in most cases since negligible residual deformation can be accepted. This study aims to present a new brace which consists of buckling restrained brace as energy dissipator and carbon fiber composite cables (CFCCs) for providing additional post-yield stiffness and self-centering force. Loss of post-tensioning force and change in stiffness are investigated experimentally for CFCC coupons. Three BRBs with post-tensioned carbon fiber composite cables (PT-BRB) are designed for this experimental study. One of the PT-BRBs is designed to have bilinear behavior with relatively high post-yield stiffness while the other two specimens use partially self-centering BRBs with different levels of post-tensioning force. A numerical study is further conducted to compare with the experimental results. Special emphasis is given on the impact of post-tensioning force. The experimental study shows that CFCCs achieve to increase post-yield stiffness of the buckling restrained braces developed herein. A stable partially self-centering behavior is possible as well.

Keywords: self-centering brace, buckling restrained brace, residual deformation, partially self-centering, PT-BRB

1. Introduction

In current seismic design practice according to modern codes, under a design basis earthquake (DBE), structural elements of a building are allowed to experience some damage as long as the human life is assured. In some circumstances, buildings may not be operational and this has a great impact on economy [1] and environment [2]. Alternatively, seismic energy dissipators help buildings to mostly remain elastic even after a devastating earthquake. Buckling restrained braces (BRBs) are one of widely accepted seismic dampers around the world (such as Turkey, Japan, USA, Taiwan, Canada, New Zealand etc.) since the first application in Japan in 1988 by Fujimoto et al. [3]. Numerical studies showed that residual deformations remain after a major earthquake when BRBs are used in buildings with pinned beam-to-column connections [4], [5]. Macrae and Kawashima [6] have proven that increasing the post-yield stiffness ratio (α) generally decreases residual deformations. In Japanese structural design practice, it is quite common to use moment resisting frames or closed frames with seismic dampers [7]. Such dual systems provide additional stiffness to the system after dampers have yielded and help to minimize residual deformations. Self-centering systems such as frames with post/pre-tensioned beam-to-column connections [8], [9], rocking frames [10], or self-centering braces [11] are proposed to have zero residual deformations. Results from a numerical study of single degree of freedom systems show that, compared to elasto-plastic behavior, zero residual deformation and similar peak drift can be obtained with flag-shaped behavior [12]. Zhu and Zhang [13] developed a self-centering brace having shape-memory alloys (SMAs). A self-centering brace consisting of friction damper and aramid tendons is developed and tested by Christopoulos et al. [14]. A similar brace concept to this is investigated by Chou and Chen [15] using steel tendons, e-glass fiber tendons, and T-700 carbon fiber tendons. A type of self-centering BRB (SC-BRB) is proposed by Miller et al. [16]. The proposed SC-BRB requires three tubes, SMA cables for enhancing self-centering mechanism and mortar filled BRB for energy dissipation. SC-BRB concept is modified by using all steel BRB and basalt fiber reinforced polymer cables [17].

This study presents an experimental investigation of a new type of brace consisting of mortar filled buckling restrained brace and post-tensioned carbon fiber composite cables (PT-BRB). Three PT-BRBs are produced and cyclically tested under different levels of post-tensioning forces. Two of them are designed to be partially self-centering brace while one of them has bilinear behavior with relatively high post yield stiffness compared to conventional BRBs.

2. Concept of PT-BRB

Preliminary design of PT-BRBs can be done with two basic assumptions: 1) Self-centering mechanism has multilinear behavior because of slight difference in compression and tension stiffness (Fig. 1a). 2) The BRB has an elastic - perfectly plastic behavior (Fig. 1b). Axial yield force ($F_{y\text{-}B}$) of brace can be obtained by combining behaviors (Fig. 1c) of SC-mechanism and BRB when BRB has yielded (δ_y). Compressive hardening adjustment factor and strain hardening ratio should be well predicted not to exceed the actuator capacity and to better calculate the energy dissipation ratio (β). The first effective stiffness can be calculated as follows:

$$K_{1-eff} = \frac{F_{y-B}}{\delta_y} \tag{1}$$

Post-yield stiffness ratio and energy dissipation ratios are major parameters for designing PT-BRBs. Post-yield stiffness ratio (α) is calculated as the ratio of post yield tension stiffness to first effective stiffness ($K_{1\text{-}eff}$ Eq. (1)) of the brace. Energy dissipation ratio (β) is a representation of self-centering characteristic of the brace. In the case β equals to 2.00 means that PT-BRB has no re-centering force and behaves similar to a conventional BRB. When β equals to 1.00 then PT-BRB has enough force to come back to its initial position. Partially self-centering brace can be obtained when β is between 1.00 and 2.00.

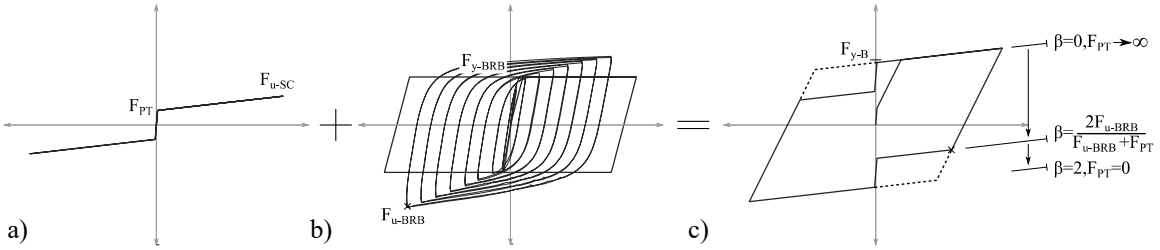

Fig. 1 - Design concept of PT-BRB a) SC mechanism, b) BRB c) total behavior

The developed PT-BRB (buckling restrained brace with post-tensioned cables) mainly consists of a steel core, two steel tubes (inner and outer), two end plates, and four symmetrically attached CFCCs. Production process of the brace is given step by step in Fig. 2a. In the first step, steel core is produced and welded to the core stiffeners (Step 1). Next, steel core is placed into inner tube, welded to left side of inner tube, and inner tube is filled with mortar to restrain buckling of the core (Step 2). Until this step, energy dissipator component (BRB) of the brace is completed. In the third step, BRB is placed in the outer tube and this time only right side of the core is welded to the outer tube (Step 3). CFCCs and endplates are placed (without welding) and post-tensioning force is applied (Step 4). The main function of self-centering mechanism is to change direction of forces on the brace for keeping CFCCs always in tension. This is achieved by having a gap in the brace both in tension and compression cases. In the initial position, tubes are in touch with the end plates. When the brace elongates under tension, end plates are pushed by the welded parts of tubes and gaps occur between the end plates and free parts of the tubes. In the case of compression, a part of forces goes to end plates through free parts of the tubes and gaps occur between the end plates and welded parts of the tubes (Fig. 2b).

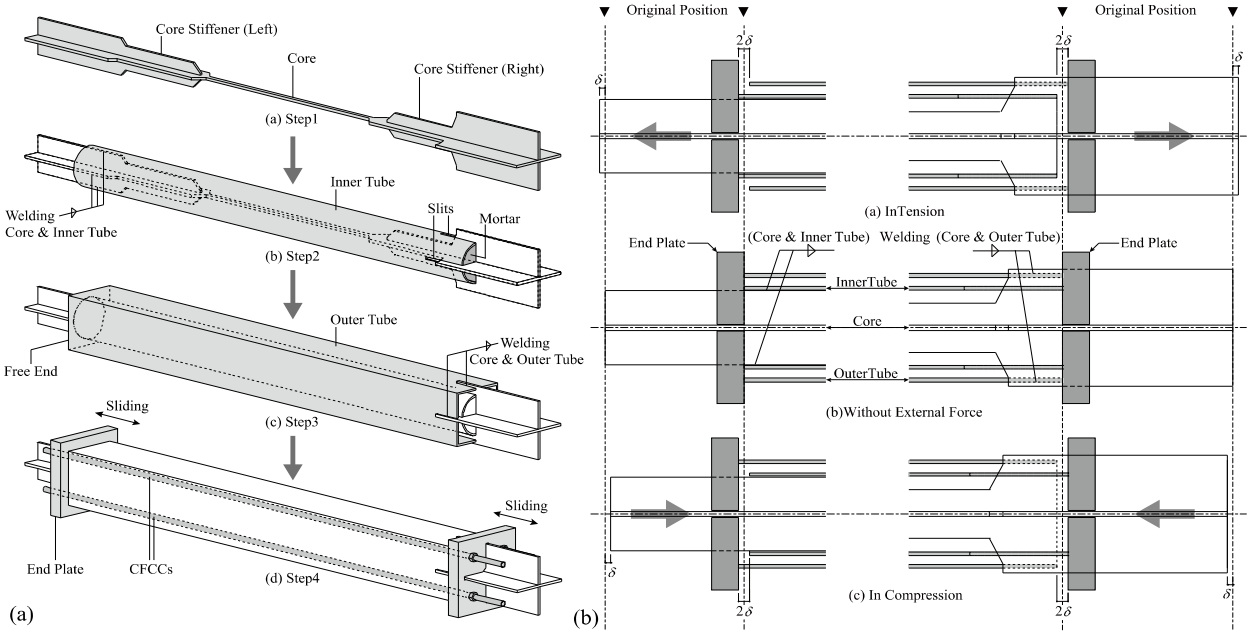

Fig. 2 - PT-BRB a) production steps, b) gap opening mechanism

3. Experimental Study

A SN400B type steel is used for core of PT-BRB. Average yield and tensile stresses of four steel coupons from monotonic tests are 283.8 MPa and 439.5 MPa, respectively.

3.1 Coupon Tests of CFCCs

CFCCs are generally used in bridge constructions or as prestressing reinforcement element in concrete [18]. Although monotonic behaviors of such members exist in literature [19], [20], cyclic behavior of CFCCs is complex and rarely published. To better understand behavior under repeated loading, CFCCs are placed into the universal testing machine using grips and steel nuts for avoiding possible slip during testing. Free length of the CFCC coupons is taken to be 380 mm (around 50 times the cross-section diameter). A loading speed of 3.75 mm/min has been performed [21]. As for the anchorage system of the coupons, a highly expansive material (HEM) and a steel sleeve have been selected. Expansion of HEM provides high pressure between the steel sleeve and carbon fiber wires, in that way, axial force on carbon fiber wires can be transferred to the steel sleeves without stress concentration [22]. As shown in test setup (Fig. 3a), two LVDTs are used to measure displacements from elongation of carbon fiber and anchor system. Loading protocol is adopted from FEMA 461 [24] (Fig. 3b) as in a study conducted by Bruce and Eatherton [23]. While CFCC-0 has no pre-tensioning force, CFCC-11.4 and CFCC19 are pre-tensioned up to 15% and 20% of design breaking load, respectively.

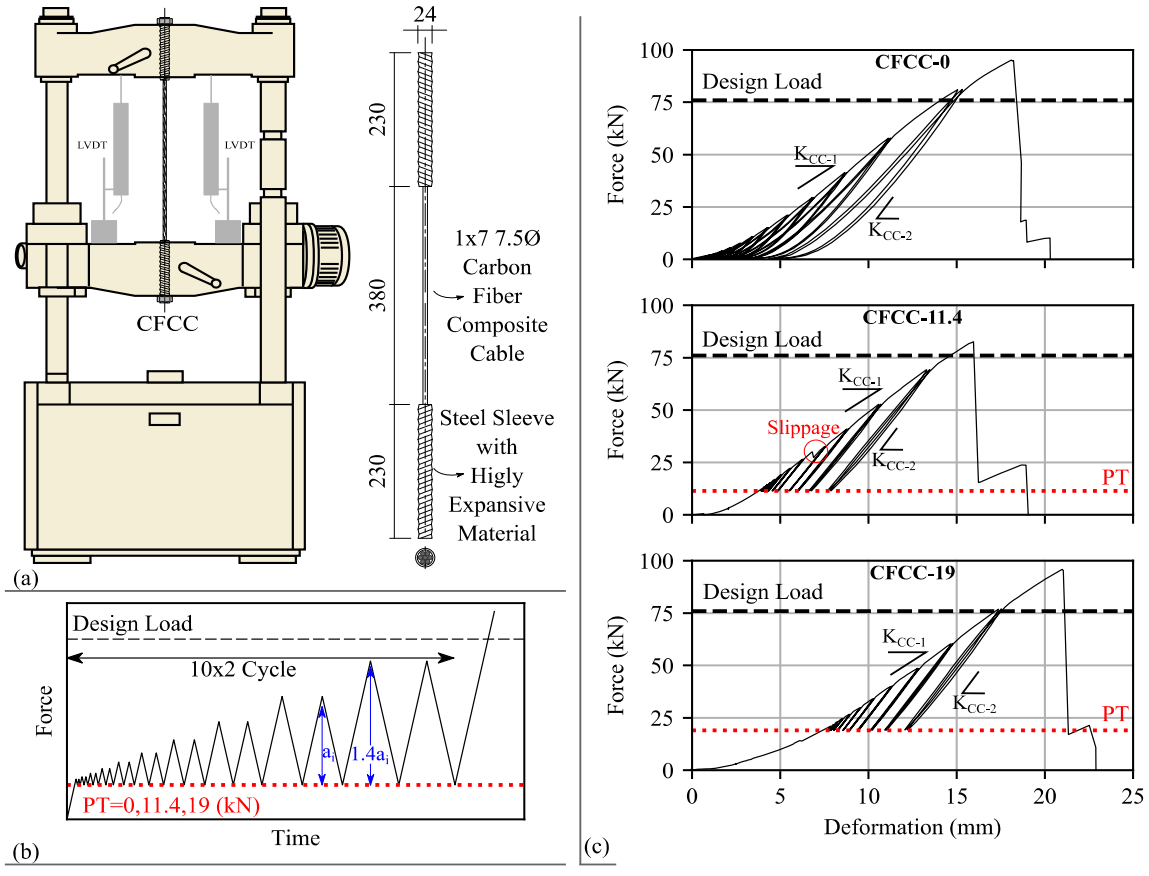

Fig. 3 - Coupon Tests of CFCC (a)test setup (b) loading protocol (c) hysteretic curves

Test results (Fig. 3c) show that CFCCs have mainly two different stiffnesses. First stiffness (K_{CC-1}) includes slippage of the anchor system or placing of cables. After cables reaches certain level of force, their stiffness increases and become more linear. This can be observed especially for CFCC-11.4 and CFCC-19. Due to no post-tensioning force, stiffness decreases when the force on cables are low. Although a slippage was recorded for CFCC 11.4, no visible damage or stiffness loss was observed. All coupons achieve to exceed design breaking loads. Average total strain and minimum linear elastic strain are obtained to be 4.83% and 2.07%, respectively. Linear elastic strain is calculated as ratio of ultimate strength to elastic stiffness (K_{CC-2}) of cables.

Even though all wires did not fracture at the same time, strength of CFCC reduced drastically after the elongation capacity has been exceeded. As shown in before (Fig. 4a) and after fracture (Fig. 4b) photos, CFCC has a brittle fracture mechanism. There was no damage on anchor system during the experiment (Fig. 4c). After CFCC coupon tests, it is decided to follow a certain path for applying post-tensioning to PT-BRBs in order to have linear stiffness during the experiments of the braces. Each cable was post-tensioned up to 70 kN and then released until the target PT-level. This method eliminates permanent deformations due to anchor system and placing of cables, additionally verify strength and linear stiffness of cables before the brace experiment.

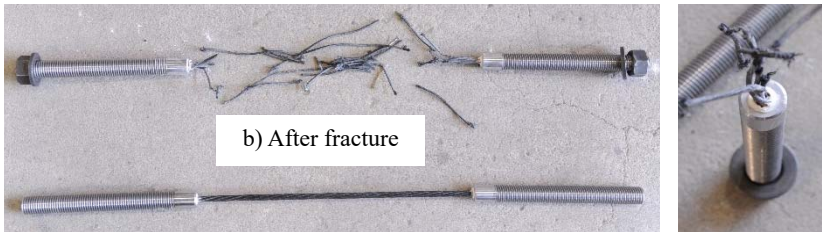

a) Before fracture

c) Anchorage after fracture

Fig. 4 - Images from CFCC coupon tests (a) before fracture (b) after fracture (c) anchorage after fracture

3.2 Cyclic Testing of PT-BRBs

Displacement controlled testing of PT-BRBs were carried out in Midarigaoka Building 2 of Tokyo Institute of Technology (TIT) by using a 500 kN capacity actuator. Simulating a typical office building with a 9-meter span, PT-BRBs are attached diagonally (25.34°) to the test frame with pinned end connections (Fig. 5a) to have only axial load on the braces. Note that work point-to-work point and yielding core lengths of braces are 3540 mm and 1000 mm, respectively.

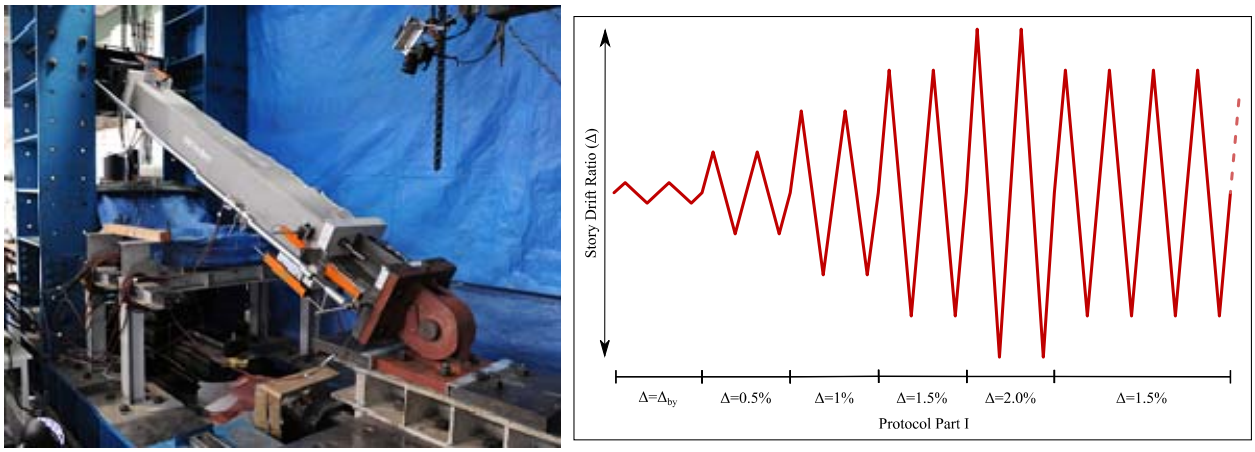

a) b)

Fig. 5– The developed self-centering brace a) PT-BRB-80 in test frame b) first part of loading protocol

Displacement responses and reaction forces of the cables are measured with 12 LVDTs and four load cells. Additionally, strain gauges are used to follow variations in tube stresses. In the first part of experiments, the AISC loading protocol for qualification of BRBs' cyclic performance [25] is applied to all specimens for a fairer comparison. Even though braces have completed the required minimum cumulative plastic deformation capacity defined in the AISC protocol, loading was continued minimum 4 cycles in the first part of loading protocol.

In the second part of loading protocol, constant amplitude loading was employed at story drift ratios of 1.5% and 2.0% for PT-BRB-56 and PT-BR-80 respectively. Due to applied low PT force, it is expected that PT-BRB-16 has more elongation capacity. Therefore, in the second part of PT-BRB-16's loading protocol, loading amplitude was increased up to 3.0%. Second part of loading protocol and loading after core fracture due to low cycle fatigue are not presented here.

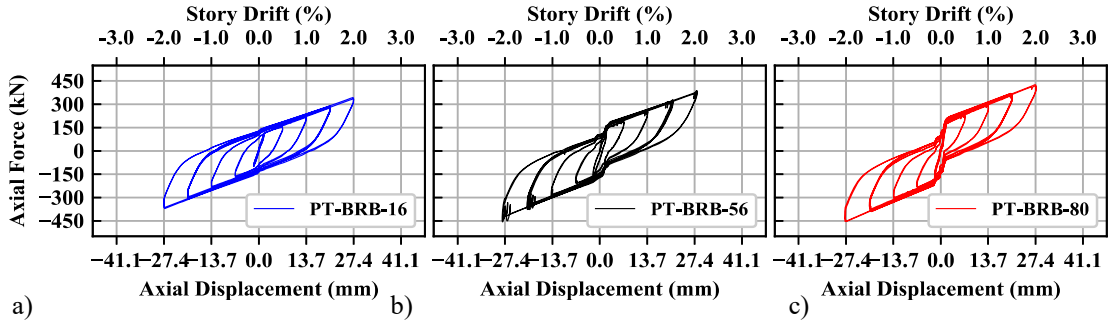

Fig. 6 - Hystereses of PT-BRBs (LP-Part I) a) PT-BRB-16 b) PT-BRB-56. c) PT-BRB-80

Axial displacement and force relation from cyclic loading tests of PT-BRBs are presented in Fig. 6. PT-BRB-16 has a bilinear behavior while partially self-centering behavior has been obtained for PT-BRB-56 and PT-BRB-80. They possess stable hystereses and achieve to complete the AISC protocol without any stiffness or strength degradation. The highest compression strength adjustment factor is calculated as 1.14 for PT-BRB-56 which is lower than the allowable limit (1.5) given in ANSI/AISC 341-16 [25]. Energy dissipation ratios (β) at 2% of story drift level are 1.93, 1.59 and 1.35 for PT-BRB-16, PT-BRB-56, and PT-BRB-80 respectively. PT-BRBs have higher post-yield stiffness when compared to conventional BRBs.

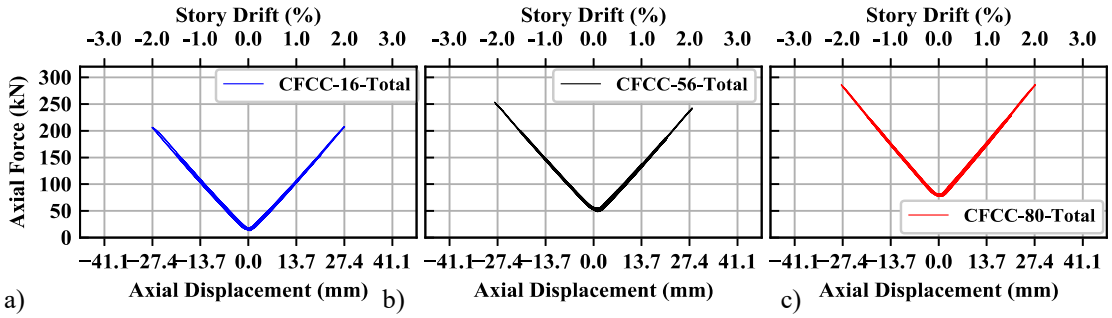

Fig. 7 - Hystereses of CFCCs (LP-Part I) a) CFCC-16 b) CFCC-56 c) CFCC-80

Hystereses of sum of CFCCs of PT-BRBs are presented in Fig. 7. Thanks to post-tensioning path, linear behavior is obtained for all specimens. Loss of post-tensioning forces are 13%, 4% for PT-BRB-56 and PT-BRB-80, respectively. PT-BRB-16 losts 6.81 kN of its post-tensioning force (16.34 kN) without

significant stiffness degradation. Peak elastic strain of (for PT-BRB-80s) CFCCs reached 1.55% at the first part of loading protocol.

4. Numerical Model

Numerical model of braces (Fig. 8) is created with Openseespy [26] and the concept of numerical model is adopted from the study done by Eatherton et al. [27]. Cables and tubes are modelled as truss elements and force based fiber element is assigned to the steel core. Elastic beam-column element is used for transition and end connection parts of the BRB. Gap opening behavior is simulated by using multi-point constraints and zero length elements. SteelMPF material model is selected in the analyses. Yield strength (σ_y=317.87 MPa), initial tangent modulus (E_0=217.8 GPa), strain hardening ratios (b_p=0.003, b_n=0.018,), initial value of the curvature parameter (R_0=15), curvature degradation parameters (c_{R1}=0.8, c_{R2}=0.0015), isotropic hardening parameters (a_1=0.024, a_2=1, a_3=0.020, a_4=1) are calibrated to match with the experimental data. Comparison between numerical and experimental force-displacement relation (Fig. 9) shows that numerical model can well predict hystereses of PT-BRBs.

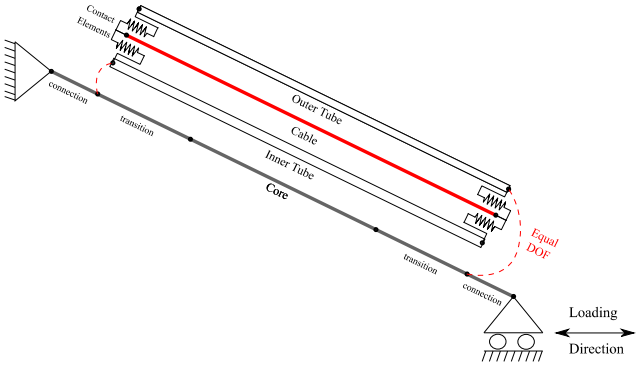

Fig. 8 – Numerical model for the brace

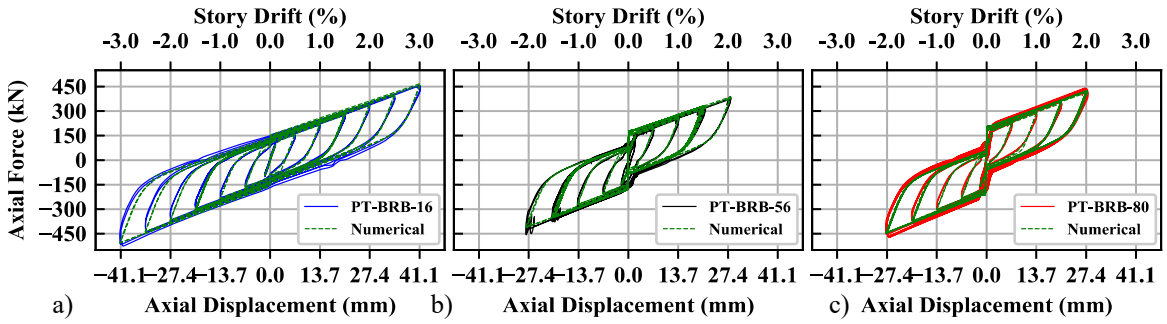

Fig. 9 - Comparison between numerical and experimental hystereses until fracture a) PT-BRB-16 b) PT-BRB-56. c) PT-BRB-80

5. Conclusions

All CFCC coupons achieve to exceed design load without any failure on the anchor system. Permanent deformation and nonlinear behavior due to placing of wires or slippage on anchor system are highly effective on self-centering behavior. Therefore, it is recommended to follow a post-tensioning path to eliminate these

drawbacks. Tests of braces showed that recommended post-tensioning method can provide linear behavior without any permanent deformation.

Experimental results of PT-BRB-16 (bilinear), PT-BRB-56 and PT-BRB-80 (partially self-centering behavior) showed that braces have stable hysteretic curves and have completed the AISC cyclic loading protocol for qualification of buckling restrained braces. Results obtained from the numerical model created for this study agree well with the experimental results.

6. Acknowledgements

The first author thanks the TUBITAK 2214-A International Doctoral Research Fellowship Programme for financial support during his research at Tokyo Institute of Technology. We acknowledge support of Mr. Kenichi Hayashi from Nippon Steel Engineering Co. Ltd. for the production of braces tested in this paper.

7. Copyrights

8. References

[1] E. Miranda, "Lessons Learned from the 2010 Haiti Earthquake for Performance-Based Design," *Geotech. Geol. Earthq. Eng.*, vol. 32, pp. 117–127, 2014.

[2] A. H. Buchanan and B. G. Honey, "Energy and carbon dioxide implications of building construction," *Energy Build.*, vol. 20, no. 3, pp. 205–217, 1994.

[3] M. Fujimoto, A. Wada, E. Saeki, A. Watanabe, and Y. Hitomi, "A study on the unbounded brace encased in buckling-restraining concrete and steel tube," *J. Struct. Eng.*, pp. 249–258, 1988.

[4] R. Sabelli, S. Mahin, and C. Chang, "Seismic demands on steel braced frame buildings with buckling-restrained braces," *Eng. Struct.*, vol. 25, no. 5, pp. 655–666, 2003.

[5] J. Erochko, C. Christopoulos, R. Tremblay, and H. Choi, "Residual Drift Response of SMRFs and BRB Frames in Steel Buildings Designed according to ASCE 7-05," *J. Struct. Eng.*, vol. 137, no. 5, pp. 589–599, 2011.

[6] G. A. Macrae and K. Kawashima, "Post-earthquake residual displacements of bilinear oscillators," *Earthq. Eng. Struct. Dyn.*, vol. 26, no. 7, pp. 701–716, 1997.

[7] F. Sutcu, A. Bal, K. Fujishita, R. Matsui, O. C. Celik, and T. Takeuchi, "Experimental and analytical studies of sub-standard RC frames retrofitted with buckling-restrained braces and steel frames," *Bull. Earthq. Eng.*, 2020.

[8] M. J. N. Priestley, S. (Sri) Sritharan, J. R. Conley, and S. Stefano Pampanin, "Preliminary Results and Conclusions From the PRESSS Five-Story Precast Concrete Test Building," *PCI J.*, vol. 44, no. 6, pp. 42–67, 1999.

[9] C. Christopoulos, A. Filiatrault, C.-M. Uang, and B. Folz, "Posttensioned Energy Dissipating Connections for Moment-Resisting Steel Frames," *J. Struct. Eng.*, vol. 128, no. 9, pp. 1111–1120, Sep. 2002.

[10] X. Ma *et al.*, "Large-scale shaking table test of steel braced frame with controlled rocking and energy dissipating fuses," in *9th US National and 10th Canadian Conference on Earthquake Engineering 2010, Including Papers from the 4th International Tsunami Symposium*, 2010, vol. 3, pp. 1914–1923.

[11] D. K. Nims, P. J. Richter, and R. E. Bachman, "The use of the energy dissipating restraint for seismic hazard mitigation," *Earthquake Spectra*, vol. 9, no. 3. pp. 467–489, 1993.

[12] C. Christopoulos, A. Filiatrault, and B. Folz, "Seismic response of self-centring hysteretic SDOF systems," *Earthq. Eng. Struct. Dyn.*, vol. 31, no. 5, pp. 1131–1150, May 2002.

[13] S. Zhu and Y. Zhang, "Seismic behaviour of self-centring braced frame buildings with reusable hysteretic damping brace," *Earthquake Engineering and Structural Dynamics*, vol. 36, no. 10. pp. 1329–1346, 2007.

[14] C. Christopoulos, R. Tremblay, H.-J. Kim, and M. Lacerte, "Self-Centering Energy Dissipative Bracing System for the Seismic Resistance of Structures: Development and Validation," *J. Struct. Eng.*, vol. 134, no. 1, pp. 96–107, Jan. 2008.

[15] C.-C. Chou and Y.-C. Chen, "Development of Steel Dual-Core Self-Centering Braces: Quasi-Static Cyclic Tests and Finite Element Analyses," *Earthq. Spectra*, vol. 31, no. 1, pp. 247–272, Feb. 2015.

[16] D. J. Miller, L. A. Fahnestock, and M. R. Eatherton, "Development and experimental validation of a nickel-

titanium shape memory alloy self-centering buckling-restrained brace," *Engineering Structures*, vol. 40. pp. 288–298, 2012.

[17] Z. Zhou, Q. Xie, X. C. Lei, X. T. He, and S. P. Meng, "Experimental Investigation of the Hysteretic Performance of Dual-Tube Self-Centering Buckling-Restrained Braces with Composite Tendons," *J. Compos. Constr.*, vol. 19, no. 6, pp. 1–13, 2015.

[18] N. Santoh, "CFCC (carbon fiber composite cable)," in *Fiber-Reinforced-Plastic (FRP) Reinforcement for Concrete Structures*, Elsevier, 1993, pp. 223–247.

[19] H. Kimura, K. Kawata, and M. Itabashi, "Analysis of tensile behavior of cfrp strand cables with various structures," *Adv. Compos. Mater.*, vol. 6, no. 1, pp. 19–32, 1996.

[20] H. Kimura, M. Itabashi, and K. Kawata, "Mechanical characterization of unidirectional CFRP thin strip and CFRP cables under quasi-static and dynamic tension Mechanical characterization of unidirectional CFRP thin strip and CFRP cables under quasi-static and dynamic," vol. 3046, 2012.

[21] ASTM-D7205/D7205M - 06, "ASTM-D7205 Standard Test Method for Tensile Properties of Fiber Reinforced Polymer Matrix Composite Bars," *Stand. Test Method Tensile Prop. Fiber Reinf. Polym. Matrix*, vol. i, no. Reapproved 2011, pp. 1–13, 2011.

[22] M. KHIN, "Fundamental Study On Bond and Anchorage of Continuous Fiber Reinforcing Materials," Kyushu Institute of Technology, 2001.

[23] T. L. Bruce and M. R. Eatherton, "Behavior of Post-Tensioning Strand Systems Subjected to Inelastic Cyclic Loading," *J. Struct. Eng.*, vol. 142, no. 10, p. 04016067, 2016.

[24] Applied Technology Council, "FEMA 461 / Interim Testing Protocols for Determining the Seismic Performance Characteristics of Structural and Nonstructural Components," 2007.

[25] American Institute of Steel Construction, "ANSI/AISC 341-16, Seismic Provisions for Structural Steel Buildings," *Seism. Provisions Struct. Steel Build.*, 2016.

[26] M. Zhu, F. McKenna, and M. H. Scott, "OpenSeesPy: Python library for the OpenSees finite element framework," *SoftwareX*, vol. 7, pp. 6–11, 2018.

[27] M. R. M. R. Eatherton, L. A. L. A. Fahnestock, and D. J. D. J. Miller, "Computational study of self-centering buckling-restrained braced frame seismic performance," *Earthq. Eng. Struct. Dyn.*, vol. 43, no. 13, pp. 1897–1914, 2014.

